World Journal of Gastroenterology

ORIGINAL ARTICLE

Basic Study

Development and *in vitro* study of a bi-specific magnetic resonance imaging molecular probe for hepatocellular carcinoma

Xiao-Hong Ma, Shuang Wang, Si-Yun Liu, Kun Chen, Zhi-Yuan Wu, Deng-Feng Li, Yong-Tao Mi, Long-Bin Hu, Zhong-Wei Chen, Xin-Ming Zhao

ORCID number: Xiao-Hong Ma (0000-0002-9048-8374); Shuang Wang (0000-0001-9241-2018); Si-Yun Liu (0000-0001-5611-382X); Kun Chen (0000-0003-3146-2577); Zhi-Yuan Wu (0000-0002-8814-0280); Deng-Feng Li (0000-0001-5754-3442); Yong-Tao Mi (0000-0002-8071-0621); Long-Bin Hu (0000-0002-0632-3623); Zhong-Wei Chen (0000-0002-1411-6675); Xin-Ming Zhao (0000-0001-7286-771X).

Xiao-Hong Ma, Shuang Wang, Deng-Feng Li, Yong-Tao Mi, Long-Bin Hu, Xin-Ming Zhao, Department of Diagnostic Radiology, National Cancer Center/Cancer Hospital, Chinese Academy of Medical Sciences and Peking Union Medical College, Beijing 100021, China

Si-Yun Liu, Zhong-Wei Chen, GE Healthcare (China), Beijing 100176, China

Kun Chen, Zhi-Yuan Wu, State Key Laboratory of Molecular Oncology, National Cancer Center/Cancer Hospital, Chinese Academy of Medical Sciences & Peking Union Medical College, Beijing 100021, China

Corresponding author: Xin-Ming Zhao, BM BCh, Professor, Department of Diagnostic Radiology, National Cancer Center/Cancer Hospital, Chinese Academy of Medical Sciences and Peking Union Medical College, No. 17, Panjiayuan Nanli, Chaoyang District, Beijing 100021, China. zhaoxinming@cicams.ac.cn
Telephone: +86-10-87787526
Fax: +86-10-87788836

Abstract

BACKGROUND
Hepatocellular carcinoma (HCC) ranks second in terms of cancer mortality worldwide. Molecular magnetic resonance imaging (MRI) targeting HCC biomarkers such as alpha-fetoprotein (AFP) or glypican-3 (GPC3) offers new strategies to enhance specificity and help early diagnosis of HCC. However, the existing iron oxide nanoparticle-based MR molecular probes singly target AFP or GPC3, which may hinder their efficiency to detect heterogeneous micro malignant HCC tumors < 1 cm (MHCC). We hypothesized that the strategy of double antibody-conjugated iron oxide nanoparticles which simultaneously target AFP and GPC3 antigens may potentially be used to overcome the tumor heterogeneity and enhance the detection rate for MRI-based MHCC diagnosis.

AIM
To synthesize an AFP/GPC3 double antibody-labeled iron oxide MRI molecular probe and to assess its impact on MRI specificity and sensitivity at the cellular level.

METHODS
A double antigen-targeted MRI probe for MHCC anti-AFP–USPIO–anti-GPC3 (UAG) was developed by simultaneously conjugating AFP and GPC3 antibodies to a 5 nm ultra-small superparamagnetic iron oxide nanoparticle (USPIO). At the

same time, the singly labeled probes of anti-AFP–USPIO (UA) and anti-GPC3–USPIO (UG) and non-targeted USPIO (U) were also prepared for comparison. The physical characterization including morphology (transmission electron microscopy), hydrodynamic size, and zeta potential (dynamic light scattering) was conducted for each of the probes. The antigen targeting and MRI ability for these four kinds of USPIO probes were studied in the GPC3-expressing murine hepatoma cell line Hepa1-6/GPC3. First, AFP and GPC3 antigen expression in Hepa1-6/GPC3 cells was confirmed by flow cytometry and immunocytochemistry. Then, the cellular uptake of USPIO probes was investigated by Prussian blue staining assay and *in vitro* MRI (T2-weighted and T2-map) with a 3.0 Tesla clinical MR scanner.

RESULTS
Our data showed that the double antibody-conjugated probe UAG had the best specificity in targeting Hepa1-6/GPC3 cells expressing AFP and GPC3 antigens compared with single antibody-conjugated and unconjugated USPIO probes. The iron Prussian blue staining and quantitative T2-map MRI analysis showed that, compared with UA, UG, and U, the uptake of double antigen-targeted UAG probe demonstrated a 23.3% (*vs* UA), 15.4% (*vs* UG), and 57.3% (*vs* U) increased Prussian stained cell percentage and a 14.93% (*vs* UA), 9.38% (*vs* UG), and 15.3% (*vs* U) reduction of T2 relaxation time, respectively. Such bi-specific probe might have the potential to overcome tumor heterogeneity. Meanwhile, the coupling of two antibodies did not influence the magnetic performance of USPIO, and the relatively small hydrodynamic size (59.60 ± 1.87 nm) of double antibody-conjugated USPIO probe makes it a viable candidate for use in MHCC MRI *in vivo*, as they are slowly phagocytosed by macrophages.

CONCLUSION
The bi-specific probe presents enhanced targeting efficiency and MRI sensitivity to HCC cells than singly- or non-targeted USPIO, paving the way for *in vivo* translation to further evaluate its clinical potential.

Key words: Hepatocellular carcinoma; Molecular imaging; Magnetic resonance imaging; Ultra-small superparamagnetic iron nanoparticles; Alpha-fetoprotein; Glypican-3

Core tip: The single targeting of existing hepatocellular carcinoma-targeted magnetic resonance imaging (HCC-targeted MRI) probes may weaken the detection efficiency due to biomarker associated tumor heterogeneity. Here, double antibody-conjugated ultra-small superparamagnetic iron nanoparticles (USPIO) were synthesized to simultaneously target HCC markers of alpha- fetoprotein (AFP) and glypican-3 (GPC3) antigens in Hepa1-6/GPC3 cells. Such probe showed higher cancer cell labeling efficiency than singly- or non-targeted USPIO probes by Prussian blue staining and *in vitro* MRI, indicating enhanced specificity and sensitivity of MRI diagnosis for micro hepatocellular carcinoma (MHCC). Meanwhile, USPIO with a small core (~5 nm) and hydrodynamic size (~60 nm) after antibody labelling may undergo slow phagocytosis, which could enhance liver tumor MRI contrast in the animal or clinical trial study.

INTRODUCTION

Hepatocellular carcinoma (HCC) is the major type of primary malignant liver tumor, and it has a high incidence rate and ranks second in terms of cancer mortality worldwide[1,2]. Surgical resection is one of the most effective methods for treating

HCC. However, only 10%–15% of the patients can be operated on when diagnosed, because most HCC patients present with a locally advanced stage disease or distant metastasis. It is encouraging that for micro hepatocellular carcinoma (MHCC) patients with tumors smaller than 1 cm in diameter and without lymph node metastasis and local invasion, the 5-year survival rate after radical operation can reach >70%[3,4]. Therefore, early and timely diagnosis of MHCC could help improve the success of surgery and significantly improve patients' survival rates.

Non-invasive imaging is the most convenient and effective way to diagnose MHCC in patients with no obvious clinical signs. Among the diverse clinical imaging methods, magnetic resonance imaging (MRI) is becoming one of the most important imaging techniques for clinical HCC screening, diagnosis, and therapeutic evaluation. MRI is a comprehensive imaging technique that is used without ionizing radiation and has a potential for quantitative analysis of morphological and functional imaging, based on high resolution of soft tissue and multi-sequence imaging parameters. MRI is sensitive and accurate for diagnosing typical HCCs with tumor diameters larger than 1 cm[5]. However, it is still a challenge for MRI to identify benign and malignant hepatic nodules less than 1 cm, mostly due to the low tumor contrast or lack of specificity for MR contrast agents[6].

Recent achievements in targeted molecular MR imaging offer new strategies to enhance specificity and contrast for detecting such small lesions[7-11]. One of the most commonly studied HCC-targeted MRI systems utilizes antibody (aptamer)-guided iron oxide nanoparticles as probes, which are intended to bind specifically with unique overexpressed HCC-related antigens or genes, such as alpha-fetoprotein (AFP) or glypican-3 (GPC3)[12-15]. AFP is a clinically widely used HCC serum bio-marker that is secreted from the cytoplasm. The specificity and sensitivity of AFP are 76%–96% and 40%–65%, respectively, whereas the false-positive and false-negative detection rates are approximately 40% and are easily affected by other liver diseases or tumors[16-18]. GPC3 is a heparan sulfate proteoglycan linked to the cell membrane by glycosylphosphatidylinositol. It is involved in regulating HCC cell proliferation and potentially serves as an HCC tissue biomarker[19,20]. GPC3 expression is highly specific to HCC tumors (84.6%), and its mRNA expression level is even higher than that of AFP, especially for tumors smaller than 3 cm[19,21].

However, the drawback of most existing HCC-targeted MRI molecular probes is that the singularity of the target may weaken the detection specificity and sensitivity, considering the tumor heterogeneity and false positive or false negative diagnoses associated with cancer biomarkers. Therefore, a more complex targeted probe design such as double antigen-targeted probes are well appreciated to precisely capture the molecular features of tumors[22,23] and, hence, are expected to further enhance the precision and imaging quality of small HCC or MHCC lesions.

Therefore, we developed a double antigen-targeted MRI probe for MHCC by simultaneously conjugating AFP and GPC3 antibodies to a 5 nm ultra-small superparamagnetic iron oxide nanoparticle (USPIO). USPIOs with a small core size (5 nm) were chosen because their slow phagocytosis by macrophages could make them ideal for liver tumor MRI in future *in vivo* studies or clinical trials[24-26]. The aim of the current research was to explore the feasibility of using a doubly targeted HCC MRI molecular probe for cancer labeling at the cellular level. A bi-specific USPIO probe, as well as single-targeting probes conjugated with only AFP or GPC3 antibodies and unlabeled USPIO, was prepared and studied in the murine hepatoma cell line Hepa1-6/GPC3, in terms of their selectivity towards AFP and GPC3 antigens and their T2 MRI properties *in vitro* on a 3.0 Tesla clinical scanner.

MATERIALS AND METHODS

Materials
N-succinimidyl ester-functionalized 5 nm USPIOs were from Sigma–Aldrich (catalog #747440, Saint Louis, MO, United States). AFP antibodies were purchased from Abcam Company (ab213328, Cambridge, United Kingdom) and R&D Systems, Inc. (MAB1368, Minneapolis, United States). GPC3 antibodies were obtained from Abcam (ab66596) and R&D Systems, Inc. (MAB2119, Minneapolis, United States). Other chemical reagents were from Sigma–Aldrich and were of analytical grade.

Preparation of antibody-conjugated USPIO probes
The 5 nm USPIO (abbreviated as U) was N-succinimidyl ester-functionalized, which enabled its efficient conjugation with primary amines of antibodies by amide bond formation between them. Single and double antibody-conjugated USPIOs were synthesized separately as anti-AFP–USPIO (UA), anti-GPC3–USPIO (UG), and anti-

AFP–USPIO–anti-GPC3 (UAG). For single antibody-conjugated probes, 18 mg/mL USPIO was reacted separately with AFP and GPC3 antibodies (400 µg/mL) in 1 mL phosphate-buffered solution (PBS, pH 7.4). For double antibody-conjugated probe, 18 mg/mL USPIO was reacted with equal amounts of AFP and GPC3 antibodies (400 µg/mL each) in a final volume of 1 mL. The mixture was gently stirred and allowed to react for 3 hours at room temperature. Each product was then purified by ultrafiltration with 1 ´ PBS (pH 7.4) for three cycles using 100 kDa MWCO centrifugal filter (Amicon Ultra-0.5) to remove the uncoupled antibodies. The probes were stored at 4 ºC for future experiments.

Physical characterization of USPIO probes

The morphology, average size, and size distribution of USPIO probes were characterized by transmission electron microscopy (TEM; FEI Tecnai G2 F30, United States) at an acceleration voltage of 300 kV. TEM samples were prepared by dropping each probe solution onto a 400-mesh copper grid with carbon film. The hydrodynamic diameters and zeta potential of the U, UA, UG, and UAG probes were measured by dynamic light scattering (DLS; Zetasizer Nano ZS90, Malvern Instruments Ltd., Worcestershire, United Kingdom). Each sample was diluted with double-distilled water and measured in the non-invasive back scatter (NIBS) mode at 25 ºC with a scattering angle of 173º.

To deduce transversal relaxivity $r2$ of USPIO, the transversal relaxation time T2 of USPIO water solution at different iron concentrations (0.25, 0.5, 0.75, 1, 1.5, and 2 mmol/L) were measured using a 3.0 Tesla clinical MR scanner (750W, GE Healthcare, United States) with 8-channel head coil. T2 images were acquired using spin echo (SE) sequence with different TE ranging from 10 ms to 170 ms. The parameters were set as follows: TR = 2000 ms, TE = 10, 20, 30, 40, 50, 70, 80, 90, 110, 130, 150, or 170 ms, matrix = 256 × 256, field of view (FOV) = 20 mm × 20 mm, and slice thickness/slice separation = 3 mm/3.3 mm, and NEX = 2.0.

Cell culture

The murine hepatoma cell line Hepa1-6 was purchased from ATCC (CRL-1830; Manassas, VA, United States). GPC3-expressing Hepa1-6 cell line (Hepa1-6/GPC3) was developed according to the established protocol[27] and cultured in RPMI-1640 supplemented with 10% fetal bovine serum (FBS), 1% penicillin-streptomycin, and 1 mg/mL G418 (Invitrogen, CA, United States) at 37 oC in a 5% CO_2 atmosphere.

Cell experiment procedure

Cellular experiments were performed as illustrated schematically in Figure 1. First, AFP and GPC3 antigen expression in Hepa1-6/GPC3 cells was confirmed by flow cytometry and immunocytochemistry. Then, the cellular uptake of USPIO probes was investigated by Prussian blue staining assay and *in vitro* MRI. The detailed experimental and analysis methods are described below.
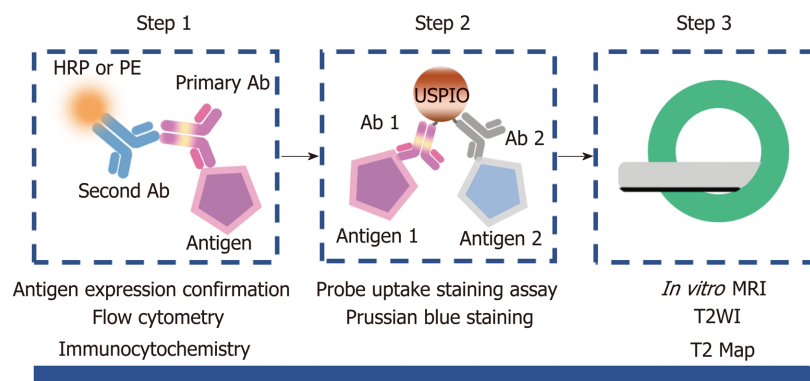
Confirmation of antigen expression

Expression of AFP and GPC3 antigens in Hepa1-6/GPC3 cells was confirmed by flow cytometry and immunocytochemistry, based on indirect fluorescence/chemical horseradish peroxidase (HRP) labeling.

Flow cytometry analysis: The rabbit anti-mouse AFP (Abcam, ab213328) and rabbit anti-mouse GPC3 (Abcam, ab66596) antibodies were used as primary antibodies, respectively, which were further binding with the secondary antibody of PE-conjugated F(ab')2-donkey anti-rabbit IgG (12-4739-81, eBioscience) for flow cytometry measurement. For intracellular staining for AFP, cells first experienced fixation and permeabilization, followed by staining with rabbit anti-mouse AFP (Abcam, ab213328) and PE-conjugated F(ab')2-donkey anti-rabbit IgG (Cat#: 12-4739-81, eBioscience). Data were acquired using an LSR-II instrument (BD, CA, United States) and analyzed using FlowJo software (Tree Star, OR, United States).

Immunocytochemistry: Hepa1-6/GPC3 cells were seeded in an 8-well chamber slide (ThermoFisher) at a density of 2 × 10⁴ cells per well and allowed to attach the coverslips for 24 hours. Following incubating cells with 1 µg/ml rabbit anti-mouse AFP monoclonal antibody (Abcam, ab213328) or rabbit anti-mouse GPC3 polyclonal antibody (Abcam, ab66596), cells were processed with the Horseradish Peroxidase (HRP) Color Development Kit (PV-9001, ZSGB-BIO, China). Cells blocked with 10% goat serum were used as a control. 3,3'-diaminobenzidine (DAB) staining was subsequently performed and hematoxylin staining was finally processed for blue cell nuclei. The 8-well chamber was then ready for bright-field optical microscopy.

Uptake of USPIO molecular probes by Hepa1-6/GPC3 cells

Figure 1 Flow of cell-based experiments. First, AFP and GPC3 antigen expression on Hepa1-6/GPC3 cells was confirmed by flow cytometry and immunocytochemistry (step 1). Next, the cellular uptake of USPIO probes was investigated by performing Prussian blue-staining assays for iron (step 2). Finally, *in vitro* MRI was performed, including T2-weighted imaging (T2WI) and T2 Map imaging (step 3). HRP: Horseradish peroxidase; PE: Phycoerythrin; Ab: Antibody; USPIO: Ultra-small superparamagnetic iron oxide; MRI: Magnetic resonance imaging; T2WI: T2-weighted imaging.

Prussian blue staining assay: Prussian blue staining was utilized to visibly assess the probes' targeting efficiency and the corresponding iron uptake by cells that were treated with four different molecular probes including U, UA, UG, and UAG. Hepa1-6/GPC3 cells were seeded in an 8-well chamber slide (ThermoFisher) at a density of 2 × 10^4 cells in each chamber and incubated for 4 h with one molecular probe at a concentration of 50 μg Fe/mL. The cells were gently rinsed three times with 1 × PBS and fixed with 4% paraformaldehyde for 30 min at RT. After washing three more times with 1 × PBS, the resulting cells were incubated with Prussian blue staining solution (Prussian Blue Staining Kit, Solarbio, China) for 15 min, washed with ultrapure water, and were then ready for microscopic observation. The cells that appeared blue were counted to determine the percentage of all cells that efficiently internalized iron or the probe. Each cell-adhering chamber was divided into a 3 × 3 matrix for stained cell counting.

In vitro **MRI:** Cells were seeded in six-well plates in 2 mL culture medium at a density of 1 × 10^6 cells/well and incubated for 24 h. Four kinds of probes (U, UA, UG, and UAG) were dissolved in fresh cell culture medium and incubated in each well with attached cells and 100 μg Fe/mL for 4 h (37 $^{\circ}$C, 5% CO$_2$). Blank cell samples were also prepared by substituting the same volume of 1 × PBS with nanoprobes. After the incubation, the cells were washed three times with 1 × PBS and detached using 150 μL trypsin per well. After centrifugation, the cells were suspended in 300 μL of 1% agarose gel in PBS and quickly transferred to a 96-well plate and were ready for MRI scanning after concretion at RT.

   In vitro MRI was performed using a 3.0 Tesla clinical MR scanner (750W, GE Healthcare, United States) with an 8-channel head coil. T2 images were acquired using spin echo (SE) sequence with different multi-echo TE time ranging from 10 ms to 170 ms. The parameters were set as follows: TR = 2000 ms; TE = 10, 20, 30, 40, 50, 70, 90, 110, 130, 150, or 170 ms; matrix = 256 × 256; FOV = 20 mm × 20 mm; and slice thickness/slice separation = 3 mm/3.3 mm; NEX = 2.0. The T2 values for each sample were fitted as an exponential decay constant from signal intensity *vs* multi-echo TE time curves.

Statistical analysis

Quantitative data are described as the mean ± SD. The Kolmogorov–Smirnov test was used to evaluate whether the continuous variables are normally distributed. Differently treated cell groups were statistically compared using the Mann–Whitney *U*-test or Student's *t*-test. Significant differences between two groups was defined as *P* < 0.05. The statistical methods of this study were reviewed by Wang SM from National Cancer Center/Cancer Hospital, Chinese Academy of Medical Sciences and Peking Union Medical College, Beijing, China.

RESULTS

Physical characterization of USPIO probes

The morphologies of U, UA, UG, and UAG probes were characterized by TEM and are illustrated in Figure 2A-D. The core diameter of the USPIOs was ~5 nm (4.88 ± 0.16 nm), as demonstrated by the TEM images (Figure 2A) and core size-distribution analysis from 147 nanoparticles (Figure 2E). TEM images of UA, UG, and UAG revealed that each probe maintained good dispersion and uniformity in size after antibody conjugation as shown in Figure 2B-D. The T2-weighted MRI contrast enhancement effects of the USPIO in water solutions are shown in Figure 2F (left column). The transversal molar relaxivity r_2 at 3.0 Tesla was extracted as 42.75 $mM^{-1} \cdot s^{-1}$ by linear regression fitting of transversal relaxation rate (1/T2) data *vs* different iron concentrations (Figure 2F, right column). The scheme used to construct the U, UA, UG, and UAG probes is illustrated in Figure 3A, and their hydrodynamic size distributions are shown in Figure 3B (which were determined by analyzing the DLS intensity-distribution data). Table 1 summarizes the hydrodynamic size and zeta potential of the U, UA, UG, and UAG probes. The hydrodynamic size of UA, UG, and UAG were 56.48 ± 0.52 nm, 54.76 ± 1.02 nm, and 59.60 ± 1.87 nm, respectively, which were lager than the unlabeled USPIOs (40.46 ± 0.53 nm). The larger size was ascribed to conjugation of the antibody to the USPIO surface, which is in accord with TEM results. Following the binding of antibodies, the negative surface charges of UA, UG, and UAG changed to –12.74 mV, –11.22 mV, and –10.23 mV, respectively, compared with –26.13 mV for unlabeled NHS-ester-functionalized USPIO.

Confirmation of antigen expression

AFP and GPC3 expression in Hepa1-6/GPC3 cells were confirmed by flow cytometry and immunocytochemistry.

The flow cytometry results are presented in Figure 4A–C. The Hepa1-6/GPC3 cells were subjected to intracellular (Figure 4A) and membrane (Figure 4B) staining with a rabbit anti-mouse AFP monoclonal antibody or isotype control of rabbit IgG, followed by incubation with a PE-conjugated anti-rabbit IgG secondary antibody. Staining with the AFP antibody was significantly higher in the cytoplasm (85.4%, mean fluorescence intensity [MFI]: 10.8) than with the cytoplasmic IgG isotype control (47.4%, MFI: 6.5; [a]$P < 0.0001$). The AFP antigen was also expressed on the membrane, based on a comparison between with the membrane isotype control and membrane AFP antibodies ([b]$P < 0.01$), as shown in Figure 4B. However, AFP was expressed mainly in the cytoplasm, with only minor membrane staining ([c]$P < 0.0001$). Membrane staining with a rabbit anti-mouse GPC3 polyclonal antibody in Hepa1-6/GPC3 cells showed greater fluorescence (71.6% positive, MFI: 11.1) than the isotype control of rabbit IgG (46.8% positive, MFI: 5.92; [d]$P < 0.01$). GPC3 was clearly expressed on the cell membrane, although the expression level was not very high. HRP-based immunological staining showed similar staining patterns for AFP and GPC3 in Hepa1-6/GPC3 cells, in which yellow-brown staining appeared (Figure 5), in contrast to the isotype control.

Uptake of USPIO molecular probes by Hepa1-6/GPC3 cells

The *in vitro* uptake of four kinds of USPIOs was investigated by Prussian blue staining and cellular MRI.

Prussian blue staining assay: Figure 6A–E shows Prussian blue-staining images of control-treated Hepa1-6/GPC3 cells and cells treated with unlabeled U, UA, UG, and UAG probes, respectively. The table in Figure 6F summarizes the percentages of stained cells treated with different kinds of USPIO probes. Cells incubated with the UAG probe possessed the highest staining percentage (~90%, *n* = 119) compared with the other three kinds of probes. The staining percentage in the UAG-treated cell group increased 23.3% (*vs* UA, *n* = 133), 15.4% (*vs* UG, *n* = 199), and 57.3% (*vs* U, *n* = 84) compared with UA-, UG-, and U-treated groups, respectively. Meanwhile, the single antibody-conjugated USPIOs also had higher cell binding efficiency relative to the unlabeled USPIO. The higher-level staining results revealed specific binding of antibody-labeled probes to the cellular antigens, AFP and GPC3.

In vitro MRI results: The double antibody-conjugated USPIO probe was designed for MRI of MHCC, with the aim of enhancing the detection specificity and sensitivity. To evaluate the targeting specificity and imaging capacity of such functionalized probe, *in vitro* MRI measurements were performed for Hepa1-6/GPC3 cell samples treated with USPIO probes. Figure 7A and B illustrates the T2WI and T2 map of Hepa1-6/GPC3 cells incubated with unlabeled USPIO, UA, UG, or UAG probes at 100 μg Fe/mL. The mean intensity for these four kinds of cell samples *vs* the corresponding TE values was plotted to calculate T2 values by exponential fitting (Figure 7C). The derived T2 values of 154.83 ms (blank control), 118.31 ms (U), 117.2 ms (UA), 110.02

Table 1 Hydrodynamic size and zeta potential of different ultra-small superparamagnetic iron oxide probes

| USPIO probe	Hydrodynamic size (nm)	Zeta potential (mV)
USPIO	40.46 ± 0.53	-26.13
Anti-AFP-USPIO	56.48 ± 0.52	-12.74
Anti-GPC3-USPIO	54.76 ± 1.02	-11.22
Anti-AFP-USPIO-anti-GPC3	59.60 ± 1.87	-10.23

USPIO: Ultra-small superparamagnetic iron oxide.

ms (UG), and 99.7 ms (UAG) are summarized in the inset table of Figure 7C. The largest reduction of the T2 value was observed with UAG-treated cell samples, which showed a 14.93%, 9.38%, and 15.3% reduction compared with UA, UG, and unlabeled USPIO, respectively. According to the darkest T2-weighted image of UAG-treated cells in Figure 7A, the results indicated that the largest amounts of iron or USPIO were bound to or internalized in Hepa1-6/GPC3 cells *via* the targeted antigens. In addition, comparing the T2 imaging results between double and single antibody-conjugated probes suggested that the double antibody-labeled USPIO probe showed enhanced binding efficiency.

DISCUSSION

The performance of double antibody-conjugated USPIO binding to cells was studied to examine the antigen-targeting ability and the potential as MRI probes for HCC.

Based on simultaneous expression of AFP and GPC3 in Hepa1-6/GPC3 cells, it was clearly demonstrated (both by Prussian blue staining and MRI) that the targeting efficiency of the double antibody-conjugated USPIO probe was higher than that of the single antibody-conjugated probes and unlabeled USPIO. Flow cytometry demonstrated that AFP and GPC3 were expressed mainly in the cytoplasm and membrane, respectively. Referring to other cellular studies that suggested a safe USPIO dosing range of ≤100 μg Fe/mL[28,29], a moderate probe concentration of 50 μg Fe/mL and a 4-hour incubation time were chosen for Prussian blue iron staining in this study. While considering the MRI signal sensitivity, a higher probe dosage of 100 μg Fe/mL was used for the *in vitro* cellular MRI experiments. In these experimental situations, the iron-internalization difference between UAG, UA, UG, and unlabeled USPIO probes could still be distinguished by statistical analysis of the percentage of Prussian blue-stained cells and the reduction of T2 values from *in vitro* MRI. The *in vitro* MRI results showed that the UAG probe-treated cells had the most significant reduction in the T2 value, followed by the UG group that possessed a smaller T2 value than the UA group, all of which were smaller than the T2 values of the unlabeled USPIO-treated group and the blank control group. At a lower probe dosage of 50 μg Fe/mL, the Prussian blue-staining results suggested a similar variation tendency, in which the UAG-treated group demonstrated the highest percentage of blue-stained cells among all of the comparison groups. Thus, three points can be discerned. First, the cellular-targeting effect of USPIO probes occurred through a combination of AFP and GPC3 antibodies and the corresponding antigens. Second, the MRI sensitivity of the USPIO probes was related to the expression level of the targeted antigens, and double biomarker-labeled probes may have the potential to overcome the tumor heterogeneity and enhance the imaging sensitivity. Third, the antibody binding did not significantly influence the magnetic properties of USPIO during MRI.

Considering the effects of vascular permeability on most solid tumors and phagocytosis by the mononuclear phagocytic system, the probe's hydrodynamic size plays an important role in entering the tumor[25,26,30]. In our study, the USPIO with a small core size (~5 nm) was adopted as the platform to further conjugate with targeting biomarkers such as AFP and GPC3 antibodies. The hydrodynamic sizes of the probes ranged from 40 nm to 59.6 nm after single or double antibody conjugation to the USPIO particles. Such size range was appropriate for *in vivo* studies, as it may help avoid leakage into the blood or fast clearance and phagocytosis by macrophages rich in normal liver tissue, which could facilitate specific probe binding to tumor antigens with a low level of background signal and clearance by the immune system[24,31-33].
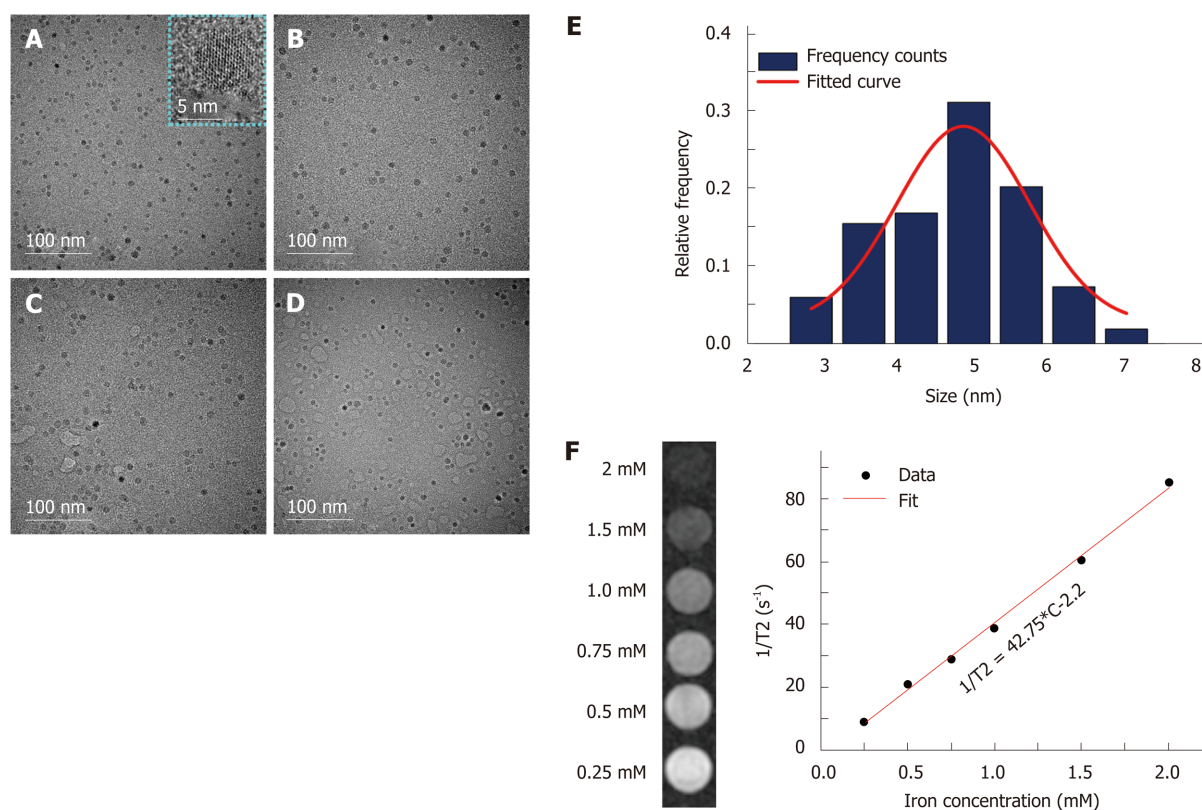
Figure 2 Physical characterization of ultra-small superparamagnetic iron oxide probes by transmission electron microscopy and magnetic resonance imaging. A-D: Transmission electron microscopy (TEM) images of ultra-small superparamagnetic iron oxide (USPIO) probes of U, UA, UG, and UAG, respectively. E: The core size distribution of USPIO with a mean diameter of 4.88 nm and a standard deviation of 0.16 nm (n = 147), as determined from the TEM images. F: T2-weighted magnetic resonance images of a series of water solutions containing different concentrations of USPIO as indicated by iron concentration (left) and linear regression fitting of the transversal relaxation rate (1/T2) data *vs* different iron concentrations for extracting the transverse relaxivity r_2 (right). UAG: Anti-AFP–USPIO–anti-GPC3; UA: Anti-AFP–USPIO; UG: Anti-GPC3–USPIO; U: Unlabeled (non-targeted) USPIO.

The present study had several limitations. First, an NHS-ester-functionalized USPIO was chosen as the basic nanoplatform for covalent conjugation with amino groups on the antibodies. Such random conjugation may block some antibody-binding sites and decrease the binding efficiency of the probes. Second, because the AFP and GPC3 antibodies had similar molecular weights (~65 kDa), the only quantification control during probe synthesis was to add the same quantity of each antibody. The exact number of labeled antibodies was not quantified, and we lacked a reference for controlling the precise ratio of the different antibodies. Third, the iron content in the study was just enough to present differences in MRI signal changes between each USPIO probe. A noticeable difference may require a further increase in the iron concentration, especially for *in vivo* experiments.

Several issues require further study in the future. In this study, the HCC biomarkers, AFP and GPC3, were chosen based on clinical considerations. The cytoplasmic expression of AFP raised the complexity of the study in terms of probe internalization. The binding of UA with AFP antigens could be inferred by comparing the Prussian blue-stained cell percentage and T2 reduction between the UA- and unlabeled USPIO-treated samples, although the differences were not significant. We hypothesized that AFP proteins secreted into the membrane play a main role in USPIO binding-induced reduction of the T2 relaxation time during *in vitro* MRI. However, the exact internalization route for such probes and whether the secreted AFP proteins contribute to UA internalization require detailed studies in the future. In addition, monoclonal antibodies against AFP and GPC3 were chosen in the study to ensure the specificity and purity. In future *in vivo* studies or investigation of cytoplasmic targeting by USPIO, small antibody fragments possessing even smaller molecular weights might generate improved results. The shrinkage of the hydrodynamic size may induce elongation of blood circulation time and shorter period of time reaching the best tumor-to-background contrast. Furthermore, the surface coating is an equally important factor for *in vivo* fate of nanoparticle-based probes. Compared with hydrophobic coatings, hydrophilic surface may help nanoparticles to avoid plasma protein adsorption and accumulation, which could lead
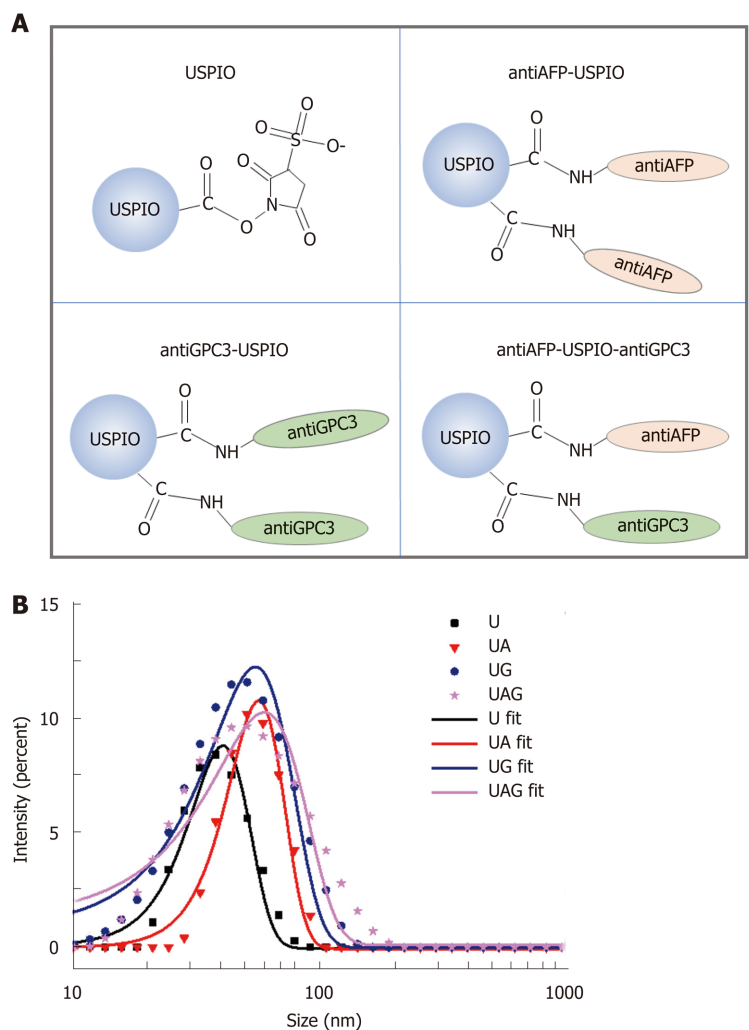
Figure 3 Hydrodynamic size distribution of antibody-conjugated ultra-small superparamagnetic iron oxides.
A: Schematic illustration of the conjugation between antibodies (anti-AFP and anti-GPC3) and USPIO-NHS ester to form single or double antibody-conjugated USPIO probes. B: Hydrodynamic size distribution of USPIO (U), anti-AFP–USPIO (UA), anti-GPC3–USPIO (UG), and anti-AFP–USPIO–anti-GPC3 (UAG). USPIO: Ultra-small superparamagnetic iron oxide; AFP: Alpha-fetoprotein; GPC3: Glypican-3; NHS ester: Succinimidyl ester.

to reticuloendothelial system (RES) or mononuclear phagocytic system recognition and uptake[34]. Therefore, to further reduce non-specific uptake of USPIO by the RES system, surface modifications, such as hydrophilic PEG coatings for the USPIO, could be also considered in the *in vivo* experiments.

In conclusion, USPIO conjugated with antibodies against two biomarkers (AFP and GPC3) were synthesized as an HCC MRI probe and evaluated using a murine hepatoma cell line expressing GPC3. The coupling of multiple antibodies did not weaken or influence the magnetic performance of USPIO, and the double antibody-conjugated USPIO probe targeted the cancer cells with higher efficiency and sensitivity than single antibody-labeled USPIO probes. Therefore, the multi-targeting strategy may be potentially applied in MRI probe design to overcome the tumor heterogeneity and enhance sensitivity for animal experiments and early clinical diagnosis of MHCC. The current study contributes preliminary data to support future *in vivo* or clinical investigations. The further validation or optimization of the probe to enhance the circulation time and suppress the background signal from normal liver, including the hydrodynamic size and surface coatings, is expected in the future *in vivo* experiments.
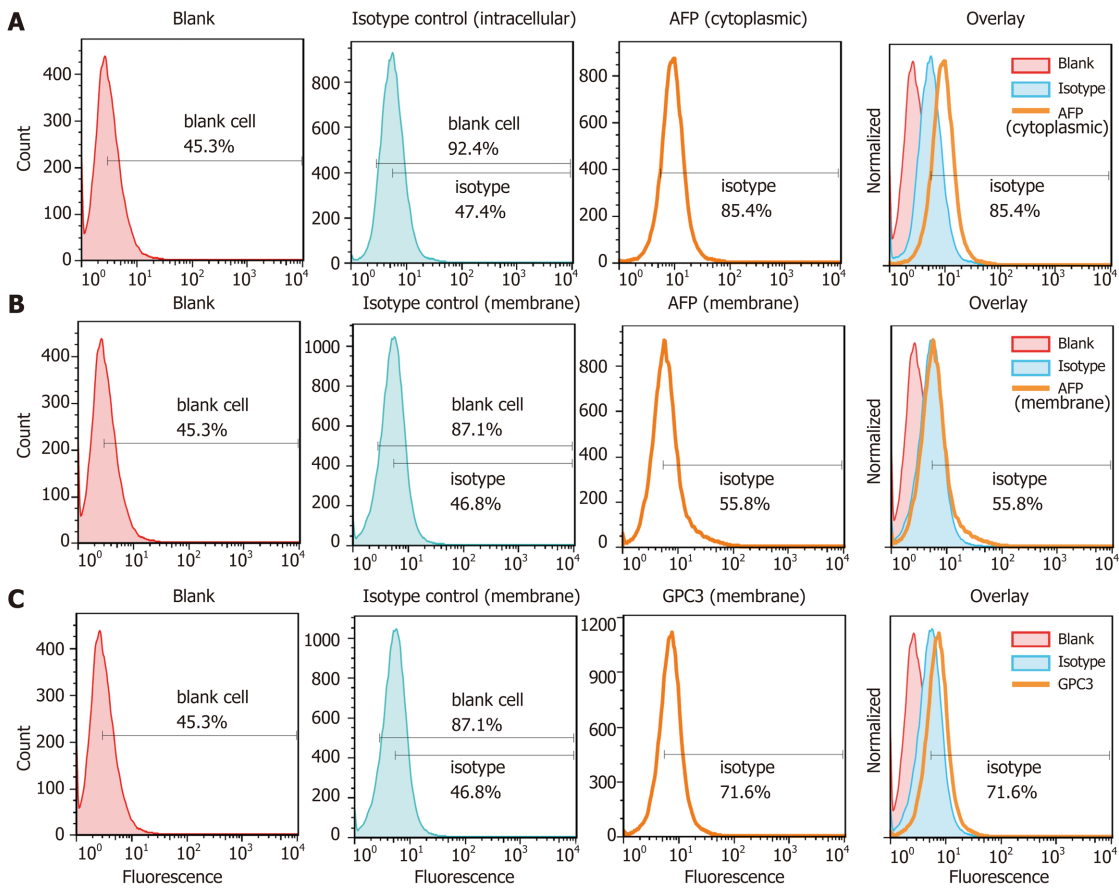
Figure 4 Detection of alpha-fetoprotein and glypican-3 antigen expression in Hepa1-6/GPC3 cells by flow cytometry. Flow cytometry data showed significantly higher alpha-fetoprotein expression in the cytoplasm (A) than in the membrane (B), compared with blank cell and IgG isotype controls. C: The positive shift of fluorescence distribution compared with isotype control illustrated higher membrane expression of the glypican-3 antigen. AFP: Alpha-fetoprotein; GPC3: Glypican-3.
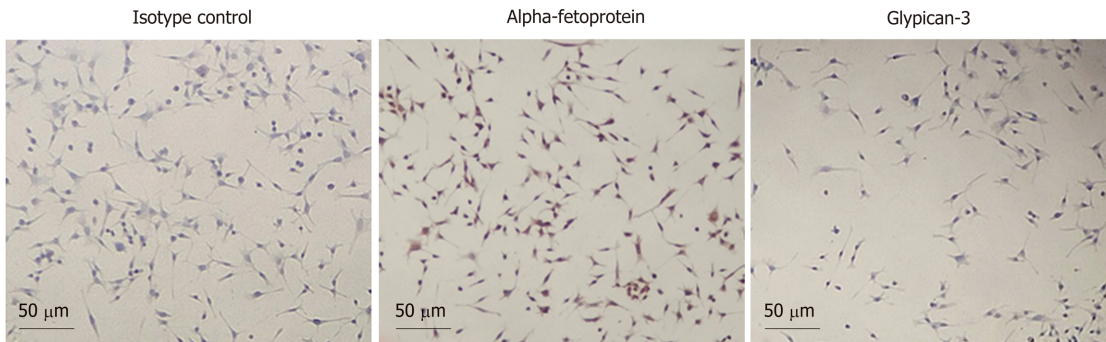
Figure 5 Cellular immunocytochemistry results. From left to right: Horseradish peroxidase-based immunological staining with IgG isotype control, anti-alpha-fetoprotein antibody, and anti-glypican-3 antibody.
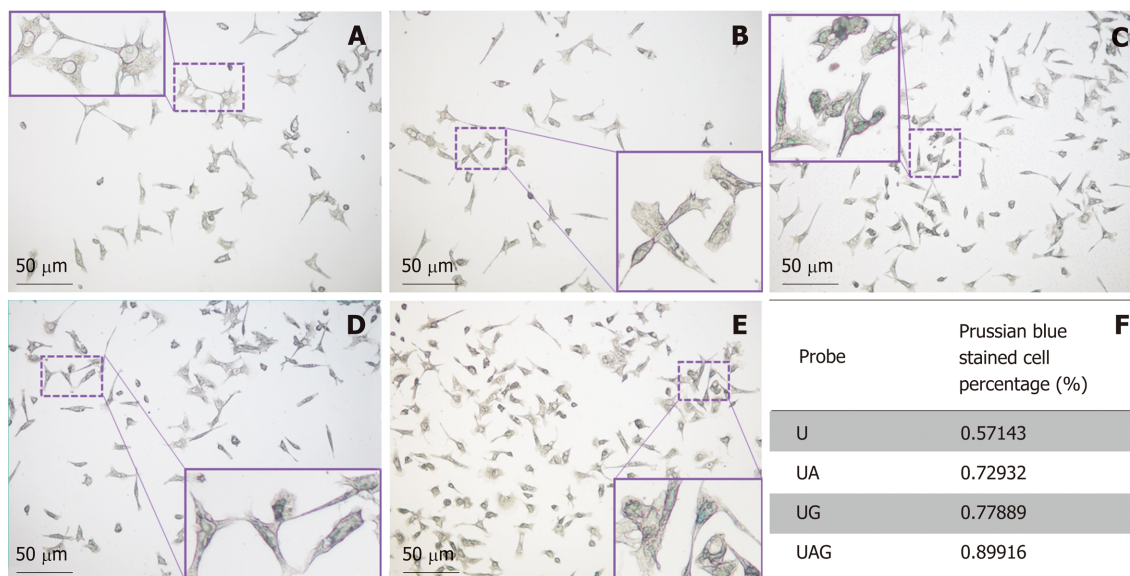
Figure 6 Prussian blue staining of Hepa1-6/GPC3 cells treated with four kinds of ultra-small superparamagnetic iron oxide probes. Prussian blue-staining images of blank Hepa1-6/GPC3 cells (A) and Hepa1-6/GPC3 cells treated with 50 μg Fe/mL of (B) USPIO (U), (C) anti-AFP–USPIO (UA), (D) anti-GPC3–USPIO (UG), or (E) anti-AFP–USPIO–anti-GPC3 (UAG). (F) Quantitation of the percentages of blue stained cells. The total counted cell number for the U, UA, UG, and UAG groups was 84, 133, 199, and 119, respectively. USPIO: Ultra-small superparamagnetic iron oxide; AFP: Alpha-fetoprotein; GPC3: Glypican-3; UAG: Anti-AFP–USPIO–anti-GPC3; UA: Anti-AFP–USPIO; UG: Anti-GPC3–USPIO; U: Unlabeled (non-targeted) USPIO.
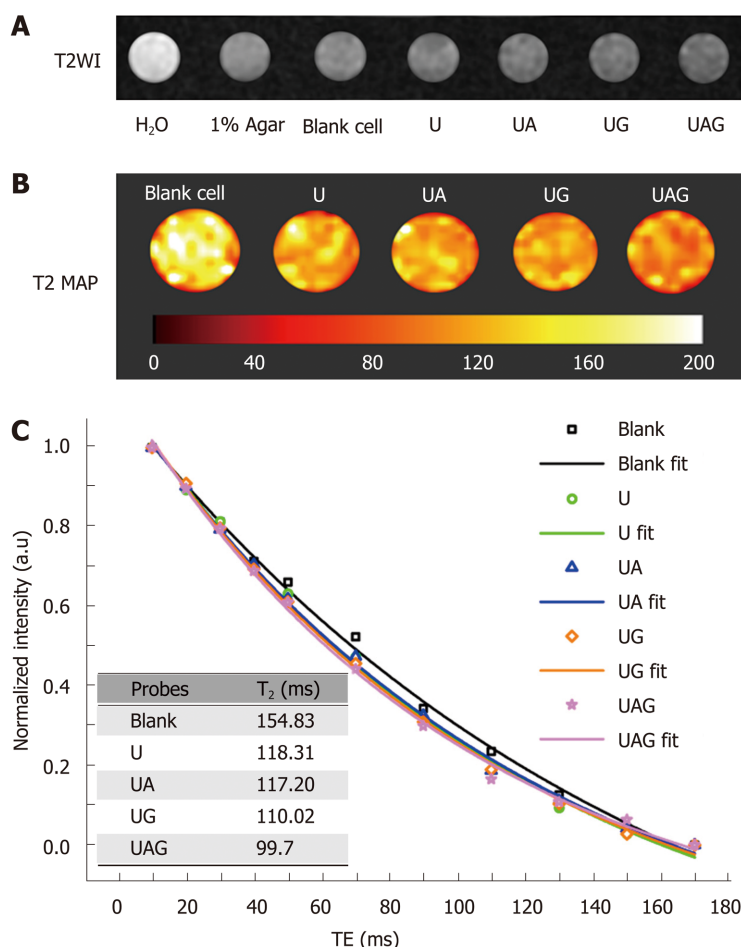
Figure 7 *In vitro* magnetic resonance imaging results demonstrating the binding efficiency and imaging properties of different ultra-small superparamagnetic iron oxide probes. A: T2WI of different samples contained in a 96-well plate. From left to right: H_2O, 1% agar, blank Hepa1-6/GPC3 cells, and hepa1-6/GPC3 cells treated with 100 μg Fe/mL USPIO (U), anti-AFP–USPIO (UA), anti-GPC3–USPIO (anti-GPC3–USPIO), or anti-AFP–USPIO–anti-GPC3 (UAG). B: Pseudocolor T2 map of cell samples treated with U, UA, UG, and UAG, respectively, compared with blank cells. T2 values are illustrated with a color bar. C: Signal

intensities of cells after different probe treatments under different TE and exponential fits for the T2 values. Inset: The fitted T2 relaxation time for cells treated with different USPIO probes (blank control, U, UA, UG, or UAG). USPIO: Ultra-small superparamagnetic iron oxide; AFP: Alpha-fetoprotein; GPC3: Glypican-3; UAG: Anti-AFP–USPIO–anti-GPC3; UA: Anti-AFP–USPIO; UG: Anti-GPC3–USPIO; U: Unlabeled (non-targeted) USPIO; T2WI: T2-weighted imaging.

ARTICLE HIGHLIGHTS

Research background
Hepatocellular carcinoma (HCC) ranks second in terms of cancer mortality worldwide. Molecular magnetic resonance imaging (MRI) targeting HCC biomarkers such as alpha-fetoprotein (AFP) or glypican-3 (GPC3) offers new strategies to enhance specificity and help early diagnosis of HCC. However, the existing iron oxide nanoparticle-based MR molecular probes singly target AFP or GPC3, which may hinder their efficiency to detect heterogeneous micro malignant HCC tumors < 1 cm (MHCC).

Research motivation
We hypothesized that the strategy of double antibody-labeled iron oxide nanoparticles which simultaneously target AFP and GPC3 antigens may potentially be used to overcome the tumor heterogeneity and enhance detection rate for MRI-based MHCC diagnosis, including the sensitivity and specificity.

Research objectives
The main objective of the current research was to synthesize an AFP/GPC3-double antibody-labeled iron oxide MR molecular probe and to assess its impact on MRI specificity and sensitivity at the cellular level. The preliminary *in vitro* data could help to optimize the key factors of MRI molecular probe design including labeled biomarkers and hydrodynamic size for future *in vivo* experiments.

Research methods
The double antigen-targeting MRI probe for MHCC anti-AFP–USPIO–anti-GPC3 (UAG) was developed by simultaneously conjugating alpha-fetoprotein (AFP) and glypican-3 (GPC3) antibodies to a 5 nm ultra-small superparamagnetic iron oxide nanoparticle (USPIO). At the same time, the singly labeled probes of anti-AFP–USPIO (UA), anti-GPC3–USPIO (UG), and non-targeted USPIO (U) were also prepared for comparison. The physical characterization including morphology (transmission electron microscopy), hydrodynamic size, and zeta potential (dynamic light scattering) was conducted for each of the probe. The antigen targeting and MR imaging ability for these four kinds of USPIO probes were studied in the GPC3-expressing murine hepatoma cell line, Hepa1-6/GPC3. First, AFP and GPC3 antigen expression in Hepa1-6/GPC3 cells was confirmed by flow cytometry and immunocytochemistry. Then, the cellular uptake of USPIO probes was investigated by Prussian blue staining assay and *in vitro* MRI (T2-weighted and T2-map) with a 3.0 Tesla clinical MR scanner. The sensitivity and specificity were evaluated based on the cellular uptake of four kinds of USPIO probes at the same dosage of iron concentration.

Research results
The *in vitro* data showed that the double antibody-conjugated probe UAG had the best specificity in targeting Hepa1-6/GPC3 cells expressing AFP and GPC3 antigens (*vs* other USPIO probes including single antibody-labeled and unlabeled USPIOs). The iron Prussian blue staining and quantitative T2-map MRI analysis showed that, compared with UA, UG, and U, the uptake of the double-targeting UAG probe demonstrated a 23.3% (*vs* UA), 15.4% (*vs* UG), and 57.3% (*vs* U) increased Prussian stained cell percentage and a 14.93% (*vs* UA), 9.38% (*vs* UG), and 15.3% (*vs* U) reduction of T2 relaxation time, respectively. Such bi-specific probe might have the potential to overcome tumor heterogeneity with enhanced sensitivity and HCC specificity. Meanwhile, the coupling of two antibodies did not influence the magnetic performance of USPIO and the relatively small hydrodynamic size (59.60 ± 1.87 nm) of the double antibody-conjugated USPIO probe makes it a viable candidate for use in MHCC MRI *in vivo*, as they are slowly phagocytosed by macrophages. AFP and GPC3 were chosen based on clinical considerations. However, the cytoplasmic expression of AFP raised the complexity of the study in terms of probe internalization. The exact internalization route for such cytoplasmic antigen-targeted probes and whether the secreted AFP proteins contribute to probe internalization require detailed studies in the future.

Research conclusions
The iron Prussian blue staining assay and *in vitro* MRI results confirmed that the bi-specific probe presents enhanced targeting efficiency and MRI sensitivity to HCC cells than singly- or non-targeted USPIO. Therefore, it implies that the multi-targeting strategy may be potentially applied in MRI probe design to enhance the malignant tumor recognition and MRI detection efficiency of MHCC for animal experiments and early clinical diagnosis.

Research perspectives
The current research utilized monoclonal antibodies against AFP and GPC3 to ensure the specificity and purity. In future *in vivo* studies or investigation of cytoplasmic targeting by

USPIO, small antibody fragments possessing smaller molecular weights might be more effective. In addition, to further reduce non-specific uptake of USPIO by the reticuloendothelial system or mononuclear phagocytic system, surface modifications, such as hydrophilic PEG coatings for the USPIO, could be also considered in the *in vivo* experiments.

REFERENCES

1   **Ferlay J**, Soerjomataram I, Dikshit R, Eser S, Mathers C, Rebelo M, Parkin DM, Forman D, Bray F. Cancer incidence and mortality worldwide: sources, methods and major patterns in GLOBOCAN 2012. *Int J Cancer* 2015; **136**: E359-E386 [PMID: 25220842 DOI: 10.1002/ijc.29210]

2   **Chen W**, Zheng R, Baade PD, Zhang S, Zeng H, Bray F, Jemal A, Yu XQ, He J. Cancer statistics in China, 2015. *CA Cancer J Clin* 2016; **66**: 115-132 [PMID: 26808342 DOI: 10.3322/caac.21338]

3   **Wang M**, Wei C, Shi Z, Zhu J. Study on the diagnosis of small hepatocellular carcinoma caused by hepatitis B cirrhosis via multi-slice spiral CT and MRI. *Oncol Lett* 2018; **15**: 503-508 [PMID: 29375718 DOI: 10.3892/ol.2017.7313]

4   **Laurent S**, Henoumont C, Stanicki D, Boutry S, Lipani E, Belaid S, Muller RN, Elst LV, MRI Contrast Agents. MRI Applications: Classification According to Their Biodistribution. SpringerBriefs in Applied Sciences and Technology. MRI Contrast Agents. Singapore: Springer 2017; 111-125

5   **Arif-Tiwari H**, Kalb B, Chundru S, Sharma P, Costello J, Guessner RW, Martin DR. MRI of hepatocellular carcinoma: an update of current practices. *Diagn Interv Radiol* 2014; **20**: 209-221 [PMID: 24808419 DOI: 10.5152/dir.2014.13370]

6   **Elsayes KM**, Hooker JC, Agrons MM, Kielar AZ, Tang A, Fowler KJ, Chernyak V, Bashir MR, Kono Y, Do RK, Mitchell DG, Kamaya A, Hecht EM, Sirlin CB. 2017 Version of LI-RADS for CT and MR Imaging: An Update. *Radiographics* 2017; **37**: 1994-2017 [PMID: 29131761 DOI: 10.1148/rg.2017170098]

7   **Zhang C**, Liu H, Cui Y, Li X, Zhang Z, Zhang Y, Wang D. Molecular magnetic resonance imaging of activated hepatic stellate cells with ultrasmall superparamagnetic iron oxide targeting integrin αvβ for staging liver fibrosis in rat model. *Int J Nanomedicine* 2016; **11**: 1097-1108 [PMID: 27051285 DOI: 10.2147/IJN.S101366]

8   **Chen YW**, Liou GG, Pan HB, Tseng HH, Hung YT, Chou CP. Specific detection of CD133-positive tumor cells with iron oxide nanoparticles labeling using noninvasive molecular magnetic resonance imaging. *Int J Nanomedicine* 2015; **10**: 6997-7018 [PMID: 26635474 DOI: 10.2147/IJN.S86592]

9   **Qiao H**, Wang Y, Zhang R, Gao Q, Liang X, Gao L, Jiang Z, Qiao R, Han D, Zhang Y, Qiu Y, Tian J, Gao M, Cao F. MRI/optical dual-modality imaging of vulnerable atherosclerotic plaque with an osteopontin-targeted probe based on Fe$_3$O$_4$ nanoparticles. *Biomaterials* 2017; **112**: 336-345 [PMID: 27788352 DOI: 10.1016/j.biomaterials.2016.10.011]

10   **Chen Q**, Shang W, Zeng C, Wang K, Liang X, Chi C, Liang X, Yang J, Fang C, Tian J. Theranostic imaging of liver cancer using targeted optical/MRI dual-modal probes. *Oncotarget* 2017; **8**: 32741-32751 [PMID: 28416757 DOI: 10.18632/oncotarget.15642]

11   **Shevtsov MA**, Nikolaev BP, Yakovleva LY, Marchenko YY, Dobrodumov AV, Mikhrina AL, Martynova MG, Bystrova OA, Yakovenko IV, Ischenko AM. Superparamagnetic iron oxide nanoparticles conjugated with epidermal growth factor (SPION-EGF) for targeting brain tumors. *Int J Nanomedicine* 2014; **9**: 273-287 [PMID: 24421639 DOI: 10.2147/IJN.S55118]

12   **Li Y**, Chen Z, Li F, Wang J, Zhang Z. Preparation and in vitro studies of MRI-specific superparamagnetic iron oxide antiGPC3 probe for hepatocellular carcinoma. *Int J Nanomedicine* 2012; **7**: 4593-4611 [PMID: 22956868 DOI: 10.2147/IJN.S32196]

13   **Li YW**, Chen ZG, Zhao ZS, Li HL, Wang JC, Zhang ZM. Preparation of magnetic resonance probes using one-pot method for detection of hepatocellular carcinoma. *World J Gastroenterol* 2015; **21**: 4275-4283 [PMID: 25892879 DOI: 10.3748/wjg.v21.i14.4275]

14   **Huang KW**, Chieh JJ, Horng HE, Hong CY, Yang HC. Characteristics of magnetic labeling on liver tumors with anti-alpha-fetoprotein-mediated Fe3O4 magnetic nanoparticles. *Int J Nanomedicine* 2012; **7**: 2987-2996 [PMID: 22787394 DOI: 10.2147/IJN.S30061]

15   **Zhao M**, Liu Z, Dong L, Zhou H, Yang S, Wu W, Lin J. A GPC3-specific aptamer-mediated magnetic resonance probe for hepatocellular carcinoma. *Int J Nanomedicine* 2018; **13**: 4433-4443 [PMID: 30122918 DOI: 10.2147/IJN.S168268]

16   **Tsuchiya N**, Sawada Y, Endo I, Saito K, Uemura Y, Nakatsura T. Biomarkers for the early diagnosis of hepatocellular carcinoma. *World J Gastroenterol* 2015; **21**: 10573-10583 [PMID: 26457017 DOI: 10.3748/wjg.v21.i37.10573]

17   **Stefaniuk P**, Cianciara J, Wiercinska-Drapalo A. Present and future possibilities for early diagnosis of hepatocellular carcinoma. *World J Gastroenterol* 2010; **16**: 418-424 [PMID: 20101765 DOI: 10.3748/wjg.v16.i4.418]

18   **Richards T**. Hepatocellular carcinoma: the potential for an effective genetic screening test .Australian Medical Student Journal 2017; Available from: http://www.amsj.org/archives/6011

19   **Chauhan R**, Lahiri N. Tissue- and Serum-Associated Biomarkers of Hepatocellular Carcinoma. *Biomark Cancer* 2016; **8**: 37-55 [PMID: 27398029 DOI: 10.4137/BIC.S34413]

20   **Wu Y**, Liu H, Ding H. GPC-3 in hepatocellular carcinoma: current perspectives. *J Hepatocell Carcinoma* 2016; **3**: 63-67 [PMID: 27878117 DOI: 10.2147/JHC.S116513]

21   **Filmus J**, Capurro M. Glypican-3: a marker and a therapeutic target in hepatocellular carcinoma. *FEBS J* 2013; **280**: 2471-2476 [PMID: 23305321 DOI: 10.1111/febs.12126]

22   **Ahmed MSU**, Salam AB, Yates C, Willian K, Jaynes J, Turner T, Abdalla MO. Double-receptor-targeting multifunctional iron oxide nanoparticles drug delivery system for the treatment and imaging of prostate cancer. *Int J Nanomedicine* 2017; **12**: 6973-6984 [PMID: 29033565 DOI: 10.2147/IJN.S139011]

23   **Kovach AK**, Gambino JM, Nguyen V, Nelson Z, Szasz T, Liao J, Williams L, Bulla S, Prabhu R. Prospective Preliminary *In Vitro* Investigation of a Magnetic Iron Oxide Nanoparticle Conjugated with Ligand CD80 and VEGF Antibody As a Targeted Drug Delivery System for the Induction of Cell Death in Rodent Osteosarcoma Cells. *Biores Open Access* 2016; **5**: 299-307 [PMID: 27843708 DOI: 10.1089/biores.2016.0020]

24   **Daldrup-Link HE**. Ten Things You Might Not Know about Iron Oxide Nanoparticles. *Radiology* 2017; **284**: 616-629 [PMID: 28825888 DOI: 10.1148/radiol.2017162759]

25   **Cortajarena AL**, Ortega D, Ocampo SM, Gonzalez-García A, Couleaud P, Miranda R, Belda-Iniesta C, Ayuso-Sacido A. Engineering Iron Oxide Nanoparticles for Clinical Settings. *Nanobiomedicine (Rij)* 2014; **1**: 2 [PMID: 30023013 DOI: 10.5772/58841]

26   **Xiao YD**, Paudel R, Liu J, Ma C, Zhang ZS, Zhou SK. MRI contrast agents: Classification and application (Review). *Int J Mol Med* 2016; **38**: 1319-1326 [PMID: 27666161 DOI: 10.3892/ijmm.2016.2744]

27   **Chen K**, Wu Z, Zang M, Wang C, Wang Y, Wang D, Ma Y, Qu C. Immunization with glypican-3 nanovaccine containing TLR7 agonist prevents the development of carcinogen-induced precancerous hepatic lesions to cancer in a murine model. *Am J Transl Res* 2018; **10**: 1736-1749 [PMID: 30018715]

28   **Mu K**, Zhang S, Ai T, Jiang J, Yao Y, Jiang L, Zhou Q, Xiang H, Zhu Y, Yang X, Zhu W. Monoclonal antibody-conjugated superparamagnetic iron oxide nanoparticles for imaging of epidermal growth factor receptor-targeted cells and gliomas. *Mol Imaging* 2015; 14 [PMID: 26044549 DOI: 10.2310/7290.2015.00002]

29   **Aliakbari M**, Mohammadian E, Esmaeili A, Pahlevanneshan Z. Differential effect of polyvinylpyrrolidone-coated superparamagnetic iron oxide nanoparticles on BT-474 human breast cancer cell viability. *Toxicol In Vitro* 2019; **54**: 114-122 [PMID: 30266435 DOI: 10.1016/j.tiv.2018.09.018]

30   **Veiseh O**, Gunn JW, Zhang M. Design and fabrication of magnetic nanoparticles for targeted drug delivery and imaging. *Adv Drug Deliv Rev* 2010; **62**: 284-304 [PMID: 19909778 DOI: 10.1016/j.addr.2009.11.002]

31   **Feng Q**, Liu Y, Huang J, Chen K, Huang J, Xiao K. Uptake, distribution, clearance, and toxicity of iron oxide nanoparticles with different sizes and coatings. *Sci Rep* 2018; **8**: 2082 [PMID: 29391477 DOI: 10.1038/s41598-018-19628-z]

32   **Longmire M**, Choyke PL, Kobayashi H. Clearance properties of nano-sized particles and molecules as imaging agents: considerations and caveats. *Nanomedicine (Lond)* 2008; **3**: 703-717 [PMID: 18817471 DOI: 10.2217/17435889.3.5.703]

33   **Pham BTT**, Colvin EK, Pham NTH, Kim BJ, Fuller ES, Moon EA, Barbey R, Yuen S, Rickman BH, Bryce NS, Bickley S, Tanudji M, Jones SK, Howell VM, Hawkett BS. Biodistribution and Clearance of Stable Superparamagnetic Maghemite Iron Oxide Nanoparticles in Mice Following Intraperitoneal Administration. *Int J Mol Sci* 2018; **19**: pii: E205 [PMID: 29320407 DOI: 10.3390/ijms19010205]

34   **Laurent S**, Saei AA, Behzadi S, Panahifar A, Mahmoudi M. Superparamagnetic iron oxide nanoparticles for delivery of therapeutic agents: opportunities and challenges. *Expert Opin Drug Deliv* 2014; **11**: 1449-1470 [PMID: 24870351 DOI: 10.1517/17425247.2014.924501]